Journal of Thermal Analysis and Calorimetry, Vol. 96 (2009) 2, 481–485

THERMAL DECOMPOSITION OF THE LAYERED DOUBLE HYDROXIDES OF FORMULA $Cu_6Al_2(OH)_{16}CO_3$ AND $Zn_6Al_2(OH)_{16}CO_3$

N. Voyer[1,2], *A. Soisnard*[1,2], *Sara J. Palmer*[1], *W. N. Martens*[1] *and R. L. Frost*[1*]

[1]Inorganic Materials Research Program, School of Physical and Chemical Sciences, Queensland University of Technology
2 George Street, Brisbane, GPO Box 2434, Queensland 4001, Australia
[2]ENSICEN, Ecole Nationale Supérieure d'Ingénieurs et Centre de Recherche, 6 Boulevard Maréchal Juin, 14050 Caen Cedex, France

Zn–Al hydrotalcites and Cu–Al hydrotalcites were synthesised by coprecipitation method and analysed by X-ray diffraction (XRD) and thermal analysis coupled with mass spectroscopy. These methods provide a measure of the thermal stability of the hydrotalcite. The XRD patterns demonstrate similar patterns to that of the reference patterns but present impurities attributed to $Zn(OH)_2$ and $Cu(OH)_2$. The analysis shows that the d003 peak for the Zn–Al hydrotalcite gives a spacing in the interlayer of 7.59 Å and the estimation of the particle size by using the Debye–Scherrer equation and the width of the d003 peak is 590 Å. In the case of the Cu–Al hydrotalcite, the d003 spacing is 7.57 Å and the size of the diffracting particles was determined to be 225 Å.

The thermal decomposition steps can be broken down into 4 sections for both of these hydrotalcites. The first step decomposition below 100°C is caused by the dehydration of some water absorbed. The second stage shows two major steps attributed to the dehydroxylation of the hydrotalcite. In the next stage, the gas CO_2 is liberated over a temperature range of 150°C. The last reactions occur over 400°C and involved CO_2 evolution in the decomposition of the compounds produced during the dehydroxylation of the hydrotalcite.

Keywords: *dehydration, dehydroxylation, hydrotalcite, thermal stability, thermogravimetric analysis*

Introduction

In nature a group of minerals is found, based upon the brucite structure ($Mg(OH)_2$), in which the divalent cation Mg^{2+} is replaced by a trivalent cation (Al^{3+}, Fe^{3+} or Cr^{3+}), resulting in a positive charge on the brucite-like surface. This positive charge is counterbalanced by anions held within the brucite interlayer. These minerals are known as hydrotalcites and layered double hydroxides (LDHs) and are fundamentally anionic clays. The structure of hydrotalcite is derived from the brucite structure ($Mg(OH)_2$) in which e.g. Al^{3+} or Fe^{3+} (pyroaurite-sjögrenite) substitutes for part of the Mg^{2+}. When LDHs are synthesised any appropriate anion can be placed in the interlayer. Included anions may be carbonate, chloride, sulphate, nitrate or any mixture of anions. This substitution creates a positive layer charge on the hydroxide layers, which is compensated by interlayer anions or anionic complexes [1, 2]. The hydrotalcite may be considered as a gigantic cation, which is counterbalanced by anions in the interlayer. In hydrotalcites a broad range of compositions are possible of the type $[M^{2+}_{1-x}M^{3+}_{x}(OH)^{x+}_{2}][A^{n}]_{x/n}\cdot yH_2O$, where M^{2+} and M^{3+} are the di- and trivalent cations in the octahedral positions within the hydroxide layers with x normally between 0.17 and 0.33. A^{n-} is an exchangeable interlayer anion [3].

Thermal analysis using thermogravimetric techniques (TG) enables the mass loss steps, the temperature of the mass loss steps and the mechanism for the mass loss to be determined [4, 5]. Thermoanalytical methods provide a measure of the thermal stability of the hydrotalcite [6–8]. The hydrotalcite series involving Zn^{2+} and Cu^{2+} mineral series is of interest because such minerals may have photocatalytic potential [9, 10]. Interest in the study of these hydrotalcites results from their potential use as catalysts, adsorbents and anion exchangers [11–15]. The reason for the potential application of hydrotalcites as catalysts rests with the ability to make mixed metal oxides at the atomic level, rather than at a particle level. Such mixed metal oxides are formed through the thermal decomposition of the hydrotalcite [16, 17]. One would expect that the potential application of hydrotalcites as catalysts will rest on reactions occurring on their surfaces.

Thermal analysis is a technique for the measurement of the thermal stability of LDH's [4–6, 18–24]. In this work we report the stability and thermal decomposition of Zn^{2+} and Cu^{2+} based LDH's with carbonate in the interlayer.

* Author for correspondence: r.frost@qut.edu.au

1388–6150/$20.00

Akadémiai Kiadó, Budapest, Hungary
Springer, Dordrecht, The Netherlands

Experimental

Synthesis of hydrotalcite minerals

Hydrotalcites with a composition of $Cu_6Al_2(OH)_{16}CO_3$ and $Zn_6Al_2(OH)_{16}CO_3$ were synthesised by the coprecipitation method. Two solutions were prepared using boiled ultra pure water: Solution 1 contained 2M NaOH and 0.125M Na_2CO_3 while solution 2 contained 0.75M Cu^{2+} ($Cu(NO_3)_2\cdot 2.5H_2O$) (or 0.75M Zn^{2+} ($Zn(NO_3)_2\cdot 6H_2O$)) and 0.25M Al^{3+} ($Al(NO_3)_3\cdot 6H_2O$). Solution 2 in the appropriate ratio was added to solution 1 using a peristaltic pump at a rate of 25 cm^3 min^{-1}, under vigorous stirring. The precipitated minerals were washed via vacuum filtration at ambient temperature with a solution of 0.1M Na_2CO_3 to remove any residual nitrate. The hydrotalcites were then centrifuged for 10 min, before being washed again with boiled ultra pure water.

X-ray diffraction

X-ray diffraction patterns were collected using a Philips X'pert wide angle X-ray diffractometer, operating in step scan mode, with CoK_α radiation (1.78897 Å). Patterns were collected in the range 3 to 75° 2θ with a step size of 0.02° and a rate of 1.2 s per step. Samples were prepared in ethanol and placed on glass slides as thin films.

Thermal analysis

Thermal decompositions of the LDH's were carried out in a TA® Instruments incorporated high-resolution thermogravimetric analyser (series Q500) in a flowing nitrogen atmosphere (80 cm^3 min^{-1}). Approximately 50 mg of sample was heated in an open platinum crucible at a rate of 2.0°C min^{-1} up to 1000°C. The TG instrument was coupled to a Balzers (Pfeiffer) mass spectrometer for gas analysis. Several gases (and isotopic analogues) and their ionic fragments were analysed including: Cl_2, CO, CO_2, HCl and H_2O.

Results and discussion

X-ray diffraction

The XRD patterns of the synthesised hydrotalcites together with the reference patterns are shown in Fig. 1. In the synthesis of hydrotalcites, it is not unexpected to have traces of impurities present either of the starting materials, by-products of the reaction or as synthesised impurities. In the case of the Zn–Al hydrotalcite the pattern matched that of the standard reference pattern together with the additional pattern of $Zn(OH)_2$. It should be remembered that the XRD

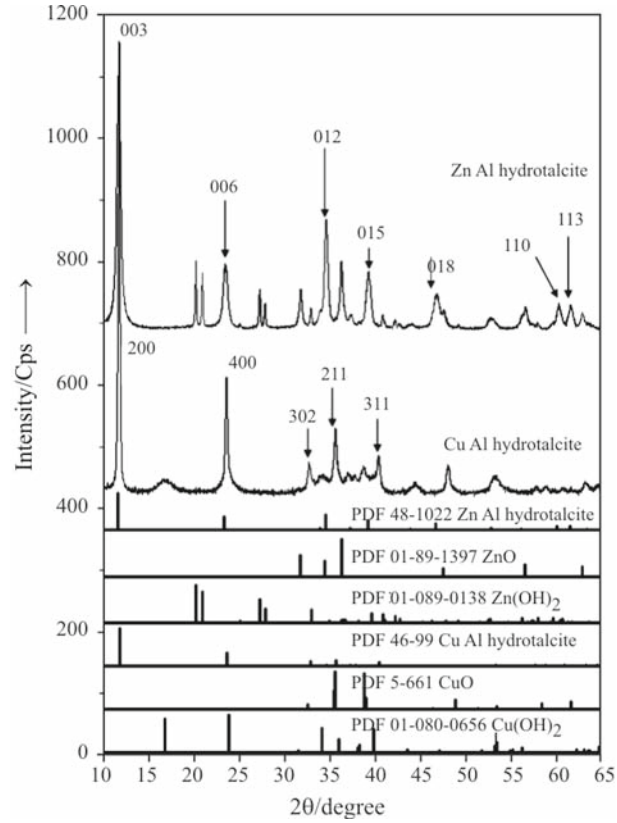

Fig. 1 X-ray diffraction patterns of the synthesized hydrotalcites

patterns are not quantitative. The $Zn(OH)_2$ is more crystalline as evidenced by the width of the peaks and thus will give a more intense pattern. It is unlikely that ZnO is present in the prepared mineral without heating. The d003 peak for the Zn–Al hydrotalcite gives a spacing of 7.59 Å. By using the Debye–Scherrer equation and the width of the d003 peak, an estimate of the particle size of the Zn–Al hydrotalcite can be made. It was found to be 590 Å.

The pattern for the Cu–Al hydrotalcite shows an identical pattern to that of the reference patterns for the Cu–Al hydrotalcite (PDF 46–99). The broad feature at about 15 degrees two theta may be attributed to an impurity of $Cu(OH)_2$. The d003 spacing for the Cu–Al hydrotalcite is 7.57 Å. The size of the diffracting particles of the Cu–Al hydrotalcite was determined to be 221 Å.

Thermogravimetric analysis

Zn–Al hydrotalcite

The thermogravimetric analysis of the Zn–Al hydrotalcite is shown in Fig. 2a and the ion current curves in Fig. 2b. The thermal decomposition steps in this analysis can be broken down into sections (a) below 100°C (b) in the 100 to 130°C temperature range

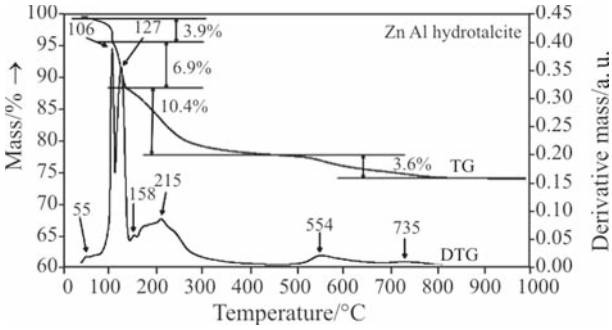

Fig. 2a TG and DTG of Zn–Al hydrotalcite

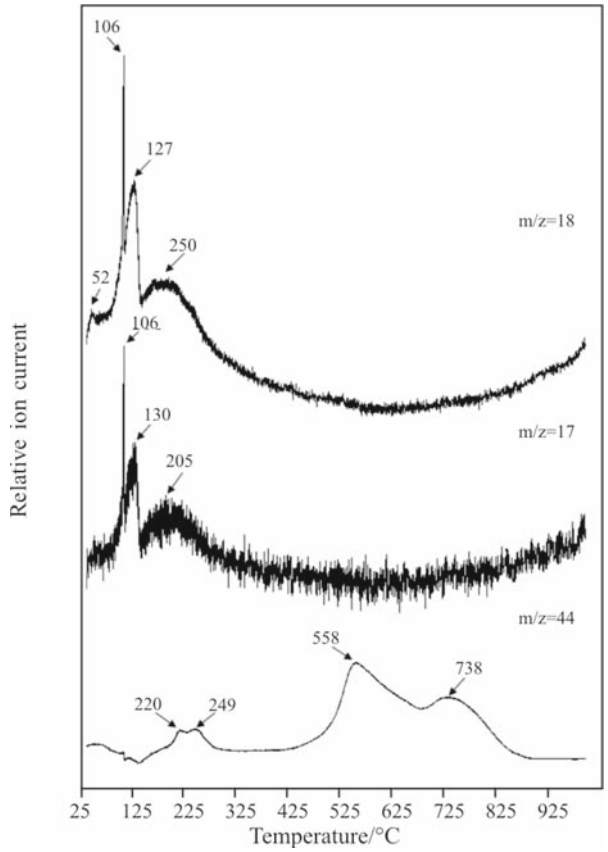

Fig. 2b Ion current curves of evolved gases of Zn–Al hydrotalcite

(c) in the 130 to 300°C temperature range and (d) in the 500 to 800°C temperature range.

(a) Below 100°C, dehydration occurs as is observed in the ion current curves where for m/z=18 a peak at ~58°C is observed. This reaction may be written as:

$$Zn_6Al_2(OH)_{16}CO_3 \cdot xH_2O \rightarrow Zn_6Al_2(OH)_{16}CO_3 + xH_2O$$

The very small peak in the DTG curve shows only a small amount of water is lost. The calculated mass loss is <0.7%. This is attributed to the mass loss of some adsorbed water.

(b) Two major thermal decomposition steps occur at 106 and 127°C with mass losses of 6.9 and 10.4%. A possible reaction is as follows:

$$Zn_6Al_2(OH)_{16}CO_3 \rightarrow y Al_2(CO_3)_3 + (1-y)Al_2O_3 + (6-x)ZnO + x ZnCO_3 + 8H_2O$$

It is noted that the m/z=17 and 18 match the DTG curves. Thus the thermal decomposition at 106 and 127°C is attributed to the dehydroxylation of the Zn–Al hydrotalcite. No loss of CO_2 is observed at these temperatures. The total mass loss for the decomposition steps at 106 and 127°C is (3.9+6.9)%. It is proposed that adsorbed water and intercalated water is lost at these temperatures. The 10.4% mass loss is observed in the temperature range between 150 and 450°C. It is suggested that dehydroxylation of the hydrotalcite takes place over this temperature range. Simultaneosuly a small amount of CO_2 is lost and the formation of metal carbonates occurs. The theoretical mass loss based upon the formula $Zn_6Al_2(OH)_{16}CO_3$ is 18.51%. Thus the experimental mass loss closely approaches that of the theoretical mass loss based upon the above formula. This data suggests that the OH units are lost before the decomposition of the $(CO_3)^{2-}$ units.

(c) The ion current curve for m/z=44 (CO_2) indicates that the evolved gas CO_2 is liberated over a temperature range centred upon 215°C. The experimental mass loss over this temperature range is 3.6%. The theoretical mass loss at 158 and 215°C is 5.65%. The difference in values may be attributed to the presence of some impurities and also some CO_2 may be liberated simultaneously with the OH units.

(d) The two higher temperature mass loss steps at 554 and 735°C also involve CO_2 evolution. It is probable that the reactions are as follows:

$$xZnCO_3 \rightarrow xZnO + xCO_2 \text{ at } 554°C$$

and

$$yAl_2(CO_3)_3 \rightarrow yAl_2O_3 + 3yCO_2 \text{ at } 735°C.$$

Most of the CO_2 is lost at these temperatures.

Cu–Al hydrotalcite

The thermogravimetric analysis of the Cu–Al hydrotalcite is shown in Fig. 3a and the ion current curves in Fig. 3b. The thermal decomposition steps in this analysis can be broken down into sections (a) below 100°C (b) in the 100 to 150°C temperature range (c) in the 150 to 350°C temperature range and (d) in the 425 to 820°C temperature range.

(a) Below 100°C, dehydration occurs as is observed in the ion current curves where for m/z=18 a peak at ~50°C is observed. This reaction may be written as:

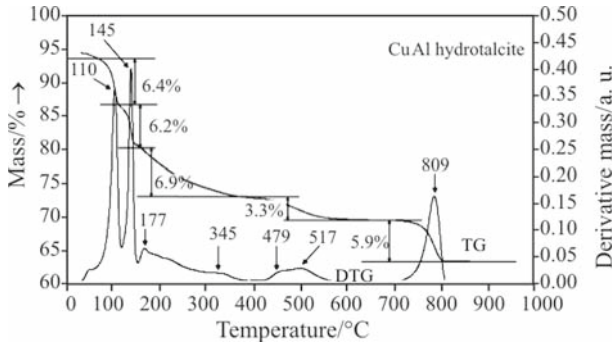

Fig. 3a TG and DTG of Cu–Al hydrotalcite

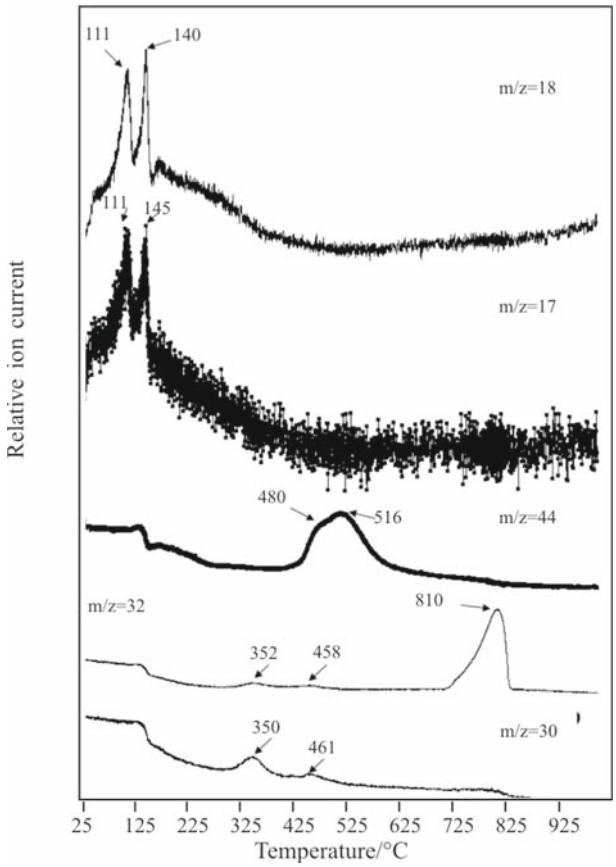

Fig. 3b Ion current curves of evolved gases of Cu–Al hydrotalcite

$$Cu_6Al_2(OH)_{16}CO_3{\cdot}xH_2O \rightarrow Cu_6Al_2(OH)_{16}CO_3+xH_2O$$

The very small peak in the DTG curve shows only a small amount of water is lost. The calculated mass loss is <0.1%. This is attributed to the loss of some adsorbed water.

(b) Two major thermal decomposition steps occur at 110 and 145°C with mass losses of 6.4 and 6.2%. A possible reaction is as follows:

$$Cu_6Al_2(OH)_{16}CO_3 \rightarrow y Al_2(CO_3)_3+(1-y)Al_2O_3+(6-x)CuO+xCuCO_3+CO_2+8H_2O$$

It is noted that the m/z=17 and 18 match the DTG curves. Thus the thermal decomposition at 110 and 140°C is attributed to the dehydroxylation of the Cu–Al hydrotalcite. Only some small amounts of CO_2 are lost at 140°C (Fig. 3b). The total mass loss for the decomposition steps at 110 and 145°C is (6.4+6.2)%=12.6%. The theoretical mass loss based upon the formula $Cu_6Al_2(OH)_{16}CO_3$ is 18.77%. Thus the experimental mass is less than the theoretical mass loss based upon the formula $Cu_6Al_2(OH)_{16}CO_3$. This data suggests that some CO_2 is evolved simultaneously with the water vapour.

(c) The ion current curve for m/z=44 (CO_2) indicates that the evolved gas CO_2 is liberated over a temperature range centred upon 513°C. The experimental mass loss over this temperature range is 3.3%. The theoretical mass loss at 158 and 215°C is 5.70%. The difference in values is attributed to the mass of CO_2 at the same time as the evolution of water vapour.

(d) A number of thermal decomposition steps are observed at 354, 479, 517°C. The shape of the DTG curve resembles that of carbonate decomposition. It is probable that the reactions are as follows:

$$xCuCO_3 \rightarrow xCuO+xCO_2 \text{ at } \sim 479°C$$

and

$$yAl_2(CO_3)_3 \rightarrow yAl_2O_3+3yCO_2 \text{ at } 517°C.$$

Conclusions

Using XRD combined with thermal analysis, the decomposition of the layered double hydroxides of formula $Cu_6Al_2(OH)_{16}CO_3$ and $Zn_6Al_2(OH)_{16}CO_3$ were studied. The XRD patterns showed that the Zn–Al hydrotalcites and Cu–Al hydrotalcites synthesised have similar patterns to that of the reference patterns of the Zn–Al hydrotalcites (PDF 48-100220) and Cu–Al hydrotalcites (PDF 46-99), but they present impurities attributed to $Zn(OH)_2$ and $Cu(OH)_2$. Both of these hydrotalcites have a close spacing respectively 7.59 and 7.57 Å, but the use of Cu reduced the particle size from 590 to 221 Å.

During the thermal decomposition of the hydrotalcites, four steps are identified, (a) below 100°C, dehydration occurs with the loss of some adsorbed water. (b) Beyond 100°C, two major thermal decomposition steps are attributed to the dehydroxylation of hydrotalcite. No loss of CO_2 is observed at these tem-

peratures. (c) The gas CO_2 is liberated over a temperature of 150°C. (d) The last reactions occur over 400°C and involved CO_2 evolution in the decomposition of the products produced during the dehydroxylation of the hydrotalcite. Both hydrotalcites showed similar thermal stability.

Acknowledgements

The financial and infra-structure support of the Queensland University of Technology Inorganic Materials Research Program of the School of Physical and Chemical Sciences is gratefully acknowledged. The Australian Research Council (ARC) is thanked for funding the thermal analysis facility.

References

1 R. M. Taylor, Clay Miner., 17 (1982) 369.
2 H. F. W. Taylor, Miner. Mag. J. Miner. Soc., (1876–1968) 37 (1969) 338–342.
3 H. C. B. Hansen and C. B. Koch, Appl. Clay Sci., 10 (1995) 5.
4 Y.-H. Lin, M. O. Adebajo, R. L. Frost and J. T. Kloprogge, J. Therm. Anal. Cal., 81 (2005) 83.
5 Y.-H. Lin, M. O. Adebajo, J. T. Kloprogge, W. N. Martens and R. L. Frost, Mater. Chem. Phys., 100 (2006) 174.
6 R. L. Frost and K. L. Erickson, J. Therm. Anal. Cal., 76 (2004) 217.
7 R. L. Frost and M. L. Weier, Thermochim. Acta, 409 (2004) 79.
8 R. L. Frost, M. L. Weier and K. L. Erickson, J. Therm. Anal. Cal., 76 (2004) 1025.
9 R. Allmann and J. D. H. Donnay, Am. Mineral., 54 (1969) 296.
10 T. Moroz, L. Razvorotneva, T. Grigorieva, M. Mazurov, D. Arkhipenko and V. Prugov, Appl. Clay Sci., 18 (2001) 29.
11 J. T. Kloprogge and R. L. Frost, Appl. Catal., A: General, 184 (1999) 61.
12 A. Alejandre, F. Medina, X. Rodriguez, P. Salagre, Y. Cesteros and J. E. Sueiras, Appl. Catal., B 30 (2001) 195.
13 J. Das and K. Parida, React. Kinet. Catal. Lett., 69 (2000) 223.
14 S. H. Patel, M. Xanthos, J. Grenci and P. B. Klepak, J. Vinyl Addit. Technol., 1 (1995) 201.
15 V. Rives, F. M. Labajos, R. Trujillano, E. Romeo, C. Royo and A. Monzon, Appl. Clay Sci., 13 (1998) 363.
16 F. Rey, V. Fornes and J. M. Rojo, J. Chem. Soc., Faraday Trans., 88 (1992) 2233.
17 M. Valcheva-Traykova, N. Davidova and A. Weiss, J. Mater. Sci., 28 (1993) 2157.
18 R. L. Frost, J. M. Bouzaid, A. W. Musumeci, J. T. Kloprogge and W. N. Martens, J. Therm. Anal. Cal., 86 (2006) 437.
19 R. L. Frost and Z. Ding, Thermochim. Acta, 405 (2003) 207.
20 R. L. Frost and K. L. Erickson, Thermochim. Acta, 421 (2004) 51.
21 R. L. Frost, W. Martens, Z. Ding and J. T. Kloprogge, J. Therm. Anal. Cal., 71 (2003) 429.
22 R. L. Frost, A. W. Musumeci, T. Bostrom, M. O. Adebajo, M. L. Weier and W. Martens, Thermochim. Acta, 429 (2005) 179.
23 R. L. Frost, A. W. Musumeci, J. T. Kloprogge, M. L. Weier, M. O. Adebajo and W. Martens, J. Therm. Anal. Cal., 86 (2006) 205.
24 R. L. Frost, M. L. Weier, M. E. Clissold, P. A. Williams and J. T. Kloprogge, Thermochim. Acta, 407 (2003) 1.

Received: April 8, 2008
Accepted: July 15, 2008
Online First: January 12, 2009

DOI: 10.1007/s10973-008-9169-x